Available online at www.sciencedirect.com
SCIENCE DIRECT
Journal of Volcanology and Geothermal Research 156 (2006) 10–22
Journal of volcanology and geothermal research
www.elsevier.com/locate/jvolgeores

The isostatic compensation of the Azores Plateau: A 3D admittance and coherence analysis

J.F. Luis *, M.C. Neves

CIMA, Universidade do Algarve, Campus de Gambelas, 8000 Faro, Portugal

Received 23 May 2003; accepted 2 March 2006
Available online 15 May 2006

Abstract

The compensation of the Azores Plateau is re-examined by means of a 3D admittance study involving computations of the admittance between the bathymetry and (1) the geoid, (2) the free air gravity and (3) the mantle Bouguer anomalies. The geoid to bathymetry relationship, rather than being analysed in the space domain, is studied in the spectral domain. In this way, the information related to the flexural response of the lithosphere is retained in the geoid to bathymetry signal and can be compared to that of the gravity to bathymetry. We find that the anomalously shallow depths of the Azores Plateau are not due to dynamic forces sustained by mantle upwelling. The Plateau is supported by a thickened crust, which mainly results from large volumes of accreted extrusives and consequent deflection of the underlying elastic plate. Both the free air gravity and the mantle Bouguer admittance point to a flexural isostatic model with a Moho depth of 12 km and an elastic thickness in the range of 3–6 km. However, the analysis of the coherency between bathymetry and the mantle Bouguer anomaly indicates that buoyant material at the base of the crust partially accounts for the uplift of the Plateau. In our best-fitting model, the average elastic thickness is 4 km and the amplitude of the buoyant load at the Moho is 1/3 of that of the surface volcanic load. Buoyancy forces at the Moho may arise from underplated material resulting from subcrustal plutonism.

Keywords: admittance; geoid interpretation; gravity; isostasy; Azores swell

1. Introduction

The Azores Plateau is a large bathymetric anomaly in the Central North Atlantic containing the triple junction between the Eurasian, African and North American plates. The Plateau is asymmetric relative to the Mid-Atlantic Ridge (MAR) and has an approximate triangular shape, as shown by the 2000-m isobath (Fig. 1). The east side of the Plateau, which roughly follows the direction of the Eurasian/African plate boundary, resulted from the intense volcanism that led to the formation of numerous seamounts and of seven of the Azores islands. The islands rise from depths locally 2000 m below to over 2000 m above sea level.

Although the Azores swell has a well-developed topographic and gravity signature, its age and origin are still uncertain. Geochemical evidence (Schilling, 1975; White et al., 1976) supports the hypothesis invoking a hotspot origin (e.g. Morgan, 1971; Sclater et al., 1975). However, Bonatti (1990) has argued against it and an alternative hypothesis is that the enhanced upwelling and magmatism is driven by plate-boundary forces (Sartoni et al., 1994). In any case, the formation of the

* Corresponding author.
E-mail address: jluis@ualg.pt (J.F. Luis).

0377-0273/$ - see front matter © 2006 Elsevier B.V. All rights reserved.
doi:10.1016/j.jvolgeores.2006.03.010

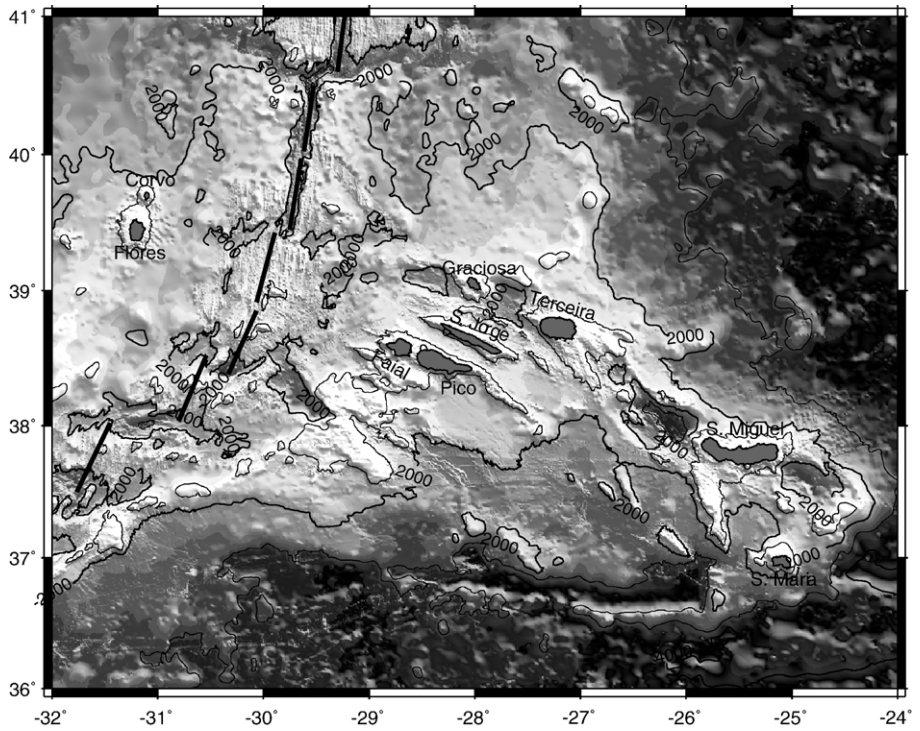

Fig. 1. Shaded illuminated bathymetry of the Azores Plateau (modified from Lourenço et al. (1988)). The heavy lines represent the MAR.

Azores Plateau seems to be connected to the progressive northward migration of the Azores triple junction (Luis et al., 1994).

Estimates of the Plateau's formation time are based on the assumption that it began to form after the jump of the triple junction to a position close to its present position, in the intersection of the MAR with the Pico–Fail islands alignment (Luis et al., 1994). According to Srivastava and Tapscott (1986) and Klitgord and Schouten (1986), the triple junction resided for a long time close to 47°N, but jumped south at about the time of magnetic anomaly 7 or 9. This places an upper limit of about 30 Ma for the onset of the Azores triple junction. It is still unclear if the triple-junction jump was triggered by a mantle plume event.

From the point of view of the hotspot theory, the Azores show some interesting features. The most striking of these is that the hotspot surface manifestation encompasses an extremely large area (the bathymetric anomaly is ~1000 km wide in the E–W direction). Also, geochemical data do not fit other hotspots trends of major- and trace-elements, and erupted basalt glass shows unusually high concentrations of water (Asimow and Langmuir, 2003). Furthermore, there is no hotspot track, i.e., the geochemical anomalies do not reveal any trace of the plate's motion relative to the hotspot reference frame. The lack of any radiometric age progression for the islands (Féraud et al., 1980), either with respect to the MAR or any other reference point further emphasizes this fact. As a result, the inferred hotspot is generally believed to be "somewhere east of the MAR", near the island of Faial (Schilling, 1991; Ito and Lin, 1995; Cannat et al., 1999). Strong arguments in favor of a mantle plume come from anomalously low seismic S-wave velocities imaged at100–200 km depth (Zhang and Tanimoto, 1993), but the resolution of tomographic studies does not allow a precise localization of the hotspot.

Directly related to the bathymetric anomaly are the free air gravity and geoid anomalies. Spectral methods employing the relationship between gravity or geoid and bathymetry are a powerful tool to investigate the compensation of swells and, hence, to determine if the anomalously shallow depths are dynamically maintained by mantle plumes (e.g., McKenzie and Bowin, 1976; McNutt, 1983) or are related to crustal anomalies. Some space–domain studies of the geoid to topography ratio in the Azores found evidence for a thermal origin of the swell (Cazenave et al., 1988; Monnereau and Cazenave, 1990). However, others found that the Plateau may be supported solely by a thickened crust (Grevemeyer, 1999). The present study re-examines the origin of the Azores swell using a more detailed and

three-dimensional analysis in the spectral domain. The response of the lithosphere in the flexural wavelength range is investigated using the relation of the free air gravity (FAA) to bathymetry. The relation of the geoid to bathymetry is used to constrain the type and depth of compensation of the Azores Plateau both in the short- and long-wavelength range. Finally, an analysis of the coherency between the Mantle Bouguer Anomaly (MBA) and the bathymetry provides additional constraints on the type and depth of loads that lead us to a unifying model that explains both the flexural and long-wavelength signal.

2. Transfer functions

Gravity and geoid anomalies reflect lateral heterogeneities in the earth's density structure. Because such anomalies often correlate with bathymetry, it became a standard approach to use the relationship between bathymetry and the gravity or geoid to gain information about the subsurface density structure and the style of isostatic compensation of the bathymetric load. Assuming that compensation occurs on a regional basis by flexure of an elastic plate, two fundamental modes of isostatic compensation can be considered: (1) the elastic plate deflects downwards in response to surface topographic loads (Fig. 2a); and (2) the topography is the response to loading within the interior or beneath the elastic plate (Fig. 2b). Negative loading, associated with thermal buoyancy forces and/or dynamic support by an upwelling plume, pushes the lithosphere from underneath, producing an uplift of the seafloor coupled to an uplift of the crust/mantle boundary, i.e., the Moho.

The transfer function $Z(k)$ between the gravity and the bathymetry in the wavenumber domain is called the "admittance function." A classical method of estimating the elastic thickness of the lithosphere is to compare the observed and theoretical admittances as a function of wavenumber or wavelength $(1/k)$. The theoretical admittances for the "load on top" (Fig. 2a) and "load from below" (Fig. 2b) models are computed from the following equations (Dorman and Lewis, 1970;

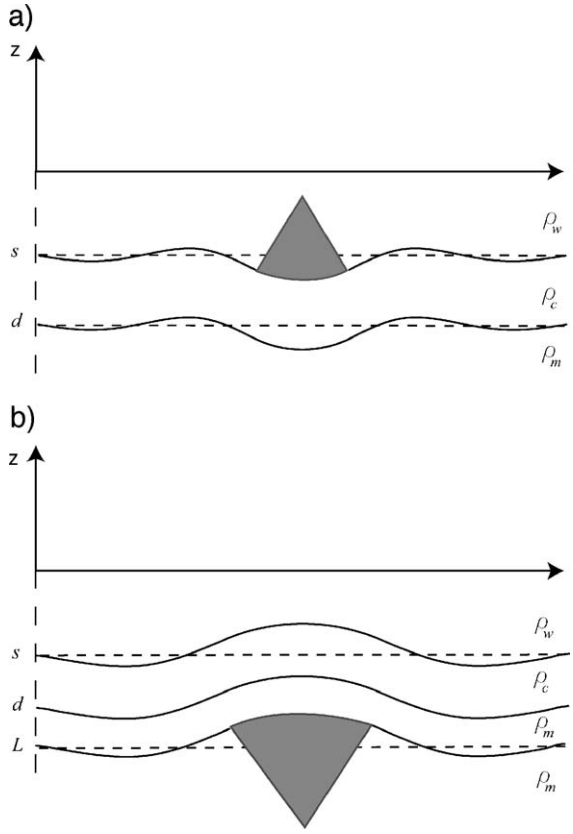

Fig. 2. Schematic model illustrating the response of an elastic plate to: a) load on top and b) load from below at depth L. Densities of seawater, crust and the mantle are ρ_w, ρ_c and ρ_m respectively. Average depths to seafloor, Moho, and swell compensation are s, d and L respectively. Note that in a) the Moho deflects downwards while in b) it deflects upwards.

McKenzie and Bowin, 1976; Banks et al., 1977; Watts, 1978; McNutt, 1979)

$$Z_{\mathrm{Top}}(k) = 2\pi G\{(\rho_c-\rho_w)[e^{-2\pi ks}-R(k)e^{-2\pi kd}]\} \quad (1)$$

$$Z_{\mathrm{Bot}}(k) = 2\pi G\{(\rho_c-\rho_w)[e^{-2\pi ks}-e^{-2\pi kL}] + (\rho_m-\rho_c)[e^{-2\pi kd}-R(k)^{-1}e^{-2\pi kL}]\} \quad (2)$$

with $R(k)$, also known as the flexural–response function, given by

$$R(k) = \left(1+\frac{D(2\pi k)^4}{g(\rho_m-\rho_c)}\right)^{-1} \quad (3)$$

The flexural rigidity of the plate is defined as $D=(ET_e^3)/[12(1-\nu^2)]$; the meaning and values of the parameters are listed in Table 1.

This method places restrictive conditions on the type of data required, namely: (1) the surveyed area needs to be several times greater than the flexural wavelength of the lithosphere, and (2) the data should sample the same tectonic province to reduce the possibility of achieving a false admittance average. Thus, the admittance will reflect an integrated T_e if provinces with different flexural rigidities are included in the same study (e.g., Louden, 1981; Forsyth, 1985).

Difficulties in interpreting the admittance arise when both loading on top and loading from below are present and/or when Z_{Top} and Z_{Bot} are similar. A combination of loading on top and loading from below occurs when surface topographic loads coexist with tectonic processes such as heating of the lithosphere and asthenosphere, plutonic intrusions or crustal underplating, which behave as internal or bottom loads. Moreover, in particular circumstances, Z_{Bot} for a strong plate may mimic Z_{Top} for a weak plate (Forsyth, 1981; Karner and Watts, 1983).

In order to combine bottom and top loading in the oceans and to estimate their relative magnitude, an alternative method uses the transfer function between the MBA and the bathymetry (Forsyth, 1985; Neumann and Forsyth, 1993). Assuming that loading occurs both at the seafloor and at the Moho, the combined theoretical admittance can be computed from (Neumann and Forsyth, 1993),

$$Z(k) = 2\pi G e^{-2\pi kd}\rho_m\theta\left(\frac{F^2+\xi}{F^2+\xi^2}\right) \quad (4)$$

where $\theta=1+D(2\pi k)^4/\rho_m g$, $\xi=1+D(2\pi k)^4/(\rho_m-\rho_c)g$ and F is the ratio of amplitude of subsurface to surface loading. As F ranges from 0 to infinity, Z varies between the top loading and bottom loading cases.

Different models with different elastic thicknesses may match the observed admittance equally well; therefore, another type of information – the coherence between MBA and bathymetry – can be used to constrain the elastic thickness and hence to distinguish different models (Forsyth, 1985). The coherence is defined as $\gamma^2=C^2/E_0E_1$, where C^2 is the power of the cross spectrum of gravity and bathymetry, and E_0 and E_1 are the power spectrum of the bathymetry and gravity, respectively. The coherence provides both a measure of the fraction of the gravity that can be predicted from the bathymetry and a means of estimating the uncertainty in $Z(k)$.

In Forsyth's method, the theoretical coherence is computed as a function of wavelength and flexural rigidity, under the assumption that surface and subsurface loadings are statistically independent. When $F=1$ (i.e., surface and subsurface loading have equal amplitude) the theoretical coherence of the MBA with bathymetry can be computed from,

$$\gamma^2 = \frac{(1+(F/\xi)^2\phi)^2}{(1+(F/\xi)^2)(1+F^2\phi^2)} \quad (5)$$

where $\phi=1+D(2\pi k)^4/(\rho_c-\rho_w)g$. Although in many cases surface and subsurface loadings are related processes (e.g., volcanic loads associated to reheating of the lithosphere) they are likely to have no significant correlation when averaged over a wide region (Forsyth, 1985).

In the wavelength range of the transition from compensated to uncompensated bathymetry, the theoretical coherence shows a pronounced drop. The comparison of the theoretical and observed coherences allows us to identify the wavelength range of that transition (drop), and infer from it the flexural rigidity of the plate. The values of F and D are thus chosen to fit both the theoretical admittance and coherence functions.

Recent studies on the isostatic compensation of North Atlantic swells and plateaus use the transfer function between the geoid and the bathymetry in the space domain (Grevemeyer, 1999; Heller and Marquart, 2002). The main advantage of this approach is that it allows inferences bearing on the kind of isostatic compensation in small and irregularly shaped areas enclosing a single swell

Table 1
Values of model parameters

E	Young modulus	0.7×10^{10} N/m^2
ν	Poisson's ratio	0.25
d	Average Moho depth	12 km
L	Mean depth of bottom load	25 km
ρ_m	Mantle density	3300 kg/m^3
ρ_c	Crustal density	2700 kg/m^3
ρ_w	Seawater density	1030 kg/m^3

or plateau (Sandwell and Renkin, 1988). Its main disadvantage is that it does not allow determining the flexural rigidity of the lithosphere, because wavelengths shorter than 600 km are not considered in this kind of analysis. Instead of using a space–domain approach, here we compute the transfer function between the geoid and the bathymetry in the wavenumber domain. This allows us to retain the wavelengths reflecting the lithosphere flexure (~100–400 km) and to use the geoid anomaly as an additional source of information on the elastic thickness of the lithosphere. The theoretical admittance functions for the geoid case can be computed from Eqs. (1) and (2) by simply replacing the term $2\pi G$ by G/gk.

In the following we use a 3D spectral approach to compute the admittance and coherence between: (1) FAA and bathymetry, (2) Geoid and bathymetry, and (3) MBA and bathymetry. Assuming that the isostatic response of the lithosphere is isotropic, an unbiased estimate of the admittance function $Z(k)$ can be calculated from the Fourier transforms of bathymetry $B(k)$ and gravity anomaly $G(k)$ or geoid $N(k)$ according to McKenzie and Bowin (1976),

$$Z_{\text{Gravity}}(k) = \frac{\langle G \cdot B^* \rangle}{\langle B \cdot B^* \rangle} \tag{6}$$

$$Z_{\text{Geoid}}(k) = \frac{\langle N \cdot B^* \rangle}{\langle B \cdot B^* \rangle} \tag{7}$$

where Z_{Geoid} and Z_{Gravity} are the admittances of geoid–bathymetry and gravity–bathymetry, respectively. The asterisk indicates the complex conjugate and the $\langle\ \rangle$ operator mean averaging over a waveband annulus of radius comprised between $|k|$ and $|k|+\Delta|k|$ in a 3D case. We compute Z_{Geoid} and Z_{Gravity} between grids using the program gravfft (ftp.ualg.pt/users/jluis/m_gmt/gravfft.tar.gz). The real part of the complex admittance, as a function of wavelength, is then compared to the theoretical admittance functions.

3. Comparison of data sets

Isostasy studies should, ideally, be made using bathymetry and gravity from two completely independent data sets. However, for most parts of the world oceans it may be very difficult to obtain adequate bathymetry without using one of the two available global bathymetric products: the Smith and Sandwell (1997) predicted bathymetry and the recent released General Bathymetric Chart of the Oceans (GEBCO) 1-min grid.

The use of the Smith and Sandwell product in admittance studies is regarded by many as a circular exercise, because this product is largely derived from the gravity anomaly data set. However, we believe that the use of Sandwell and Smith (1997) gravity and Smith and Sandwell bathymetry for isostasy studies should not be considered a circular exercise even in theory. Smith and Sandwell (1994) provide a lengthy discussion on how the band-pass filters were designed to isolate, and avoid, the band of wavelengths where the gravity–topography transfer function is a strong function of the isostatic compensation model. Thus, the bathymetric grid gets its information from gravity only at wavelengths shorter than 160 km and this is to ensure that the information comes only from the uncompensated band (Walter Smith, 2004, written communication).

The GEBCO grid is strongly dependent on GEBCO contours and, as a consequence, is very dependent on the spacing between the control data. For some parts of the world, the spacing between these points is so large that isostasy studies are not possible. Also, grids produced from contours suffer a statistical bias due to "terracing." The GEBCO grid in the Azores area, in particular, suffers

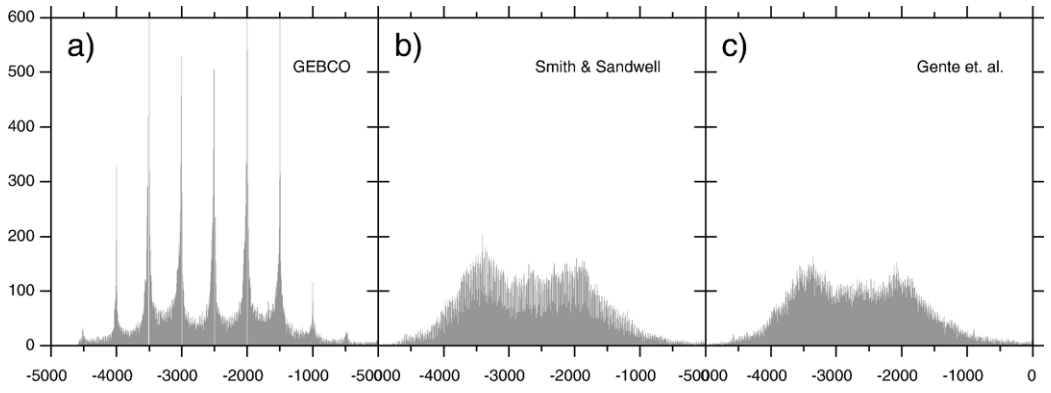

Fig. 3. Histograms of a) GEBCO, b) Smith and Sandwell (1997) and c) Gente et al. (2003) grids in the Azores area between 35–43°N and 23–33°W.

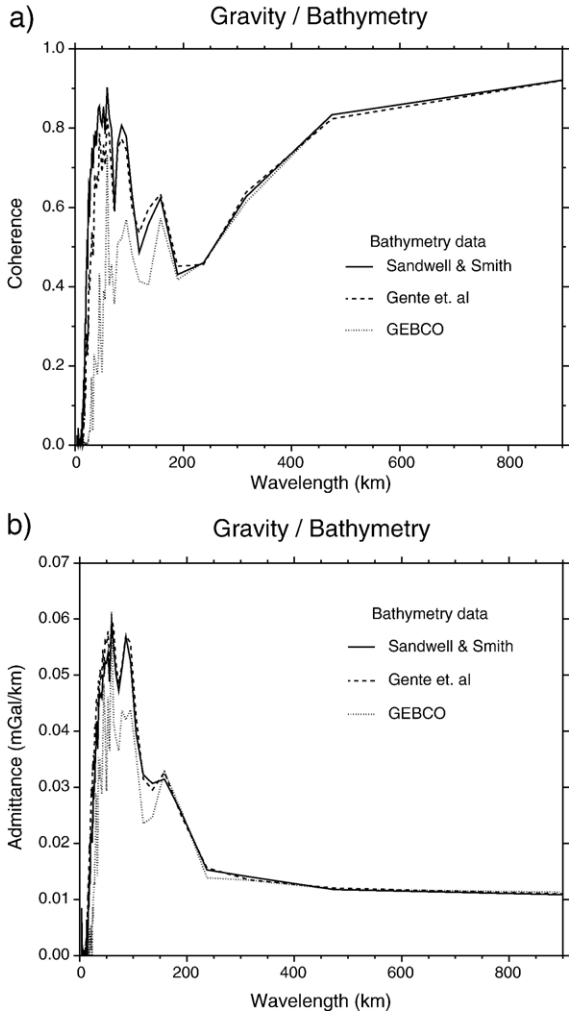

Fig. 4. a) Coherence between FAA and bathymetry compared for the three different bathymetric data sets. b) Admittance between FAA and bathymetry compared for the three different bathymetric data sets.

from an artificial frequency of depths near multiples of 500 m (Fig. 3).

We compare the performance of the Sandwell and Smith and GEBCO products in admittance studies using an independent third bathymetry grid (Gente et al., 2003). This grid is based on all available multibeam bathymetric data and on a compilation of single beam data (both classified and unclassified) provided to the authors by the French Service Hydrographique et Oceanographique de la Marine (SHOM). The final bathymetric grid was computed by Gente et al. (2003) at a grid interval of 1 km and resampled here at a grid spacing of 1 min.

The coherence and admittance between FAA and bathymetry are compared in Fig. 4a and b (respectively) for the three bathymetric data sets. For wavelengths shorter than about 150 km, Sandwell and Smith grid is the one showing the higher coherence. This is interpreted as a remnant correlation between the predicted bathymetry and the gravity data. The GEBCO grid is much noisier and shows a significantly lower coherence for wavelengths shorter than 200 km. Regarding the admittance, the Sandwell and Smith and Gente et al. grids lead to virtually indistinguishable admittance curves, demonstrating that the predicted bathymetry product can be used in admittance studies without introduction of "circularity." In contrast the GEBCO grid shows lower admittance values.

Below we use the Gente et al. (2003) grid but nothing would substantially change in our conclusions if the Sandwell and Smith predicted grid had been used. This, however, would not be the case if the GEBCO grid had been used instead, for it would lead to an underestimate of the elastic thickness.

4. FAA to bathymetry

The coherence between FAA and bathymetry (Fig. 4a) is almost everywhere above 0.5, meaning that more than half of the energy of the gravity signal can be predicted from the bathymetry. The exceptions are a small band of wavelengths around 200 km where the coherence is approximately 0.4, and the shortest wavelengths (<40 km) which are dominated by noise.

We therefore compute the admittance between the FAA and the bathymetry grids, according to Eq. (6), and consider it meaningful at all wavelengths except the

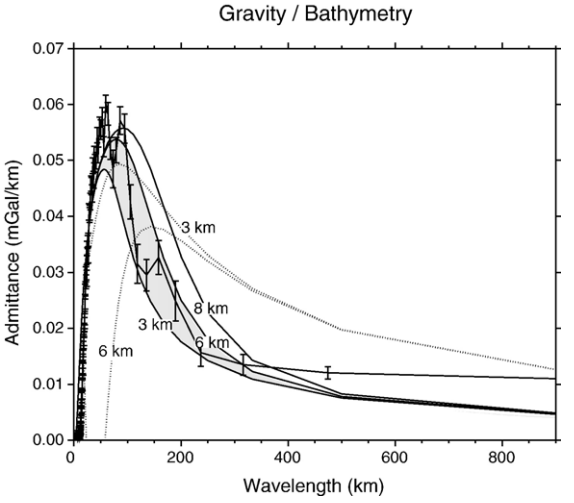

Fig. 5. FAA to bathymetry admittance. The observed admittance (solid thick line) is shown with error bars representing ±1 σ. Theoretical bottom-load models are represented by dotted lines and theoretical top-load models by solid lines. Values of 3, 6 and 8 km indicate the model elastic thickness. The compensation depth assumed for the bottom load is 25 km.

shortest. The area considered in the computation lies between 35–43°N and 23–33°W. The obtained admittance is plotted in Fig. 5 together with error bars. The error bars represent the variance of the admittance estimator, calculated according to Bendat and Piersol (2000).

The observed admittance is compared in Fig. 5 to the theoretical transfer functions of both "load on top" (solid lines) and "load from below" (dotted lines) models. The models considered are (1) "load on top" models assuming elastic thicknesses of 3, 6 and 8 km, and (2) "load from below" models assuming a mean depth of load of 25 km and elastic thicknesses of 3 and 6 km. In the wavelength range of interest (~100–400 km), "load from below" models with a mean depth of load larger than 25 km produce admittance values consistently larger than observed, so they are not plotted. The same applies to "load on top" models with elastic thicknesses larger than 8 km.

An analysis of the sensitivity of the elastic model to the values of the average crustal density and mean Moho depth has been made in a previous study (Luis et al., 1998). Based on its results, we assume a Moho mean depth of 12 km and an average crustal density of 2700 kg/m^3 in all plotted theoretical transfer functions. Other parameter values are listed in Table 1.

Fig. 5 shows that a model of loading on top with elastic thickness varying between 3 and 6 km (gray area) can explain the admittance for wavelengths up to ~300 km. For longer wavelengths, the observed admittance lies between the top- and bottom-load models, approaching asymptotically the load from below model with a mean depth of 25 km in the long-wavelength limit. The possibility of some loading from below suggested by the long-wavelength signal will be investigated later using the admittance between the MBA and the bathymetry.

5. Geoid to bathymetry

Before the admittance computation, we removed the effect of large-scale mantle dynamics in the long-wavelength geoid undulations by subtraction of a low degree and order spherical harmonic geoid representation of the EGM96 model (Lemoine et al., 1998). The coefficients from degree 10 to 25 were tapered with a cosine function to reduce artifacts from the edges of the filter (Sandwell and Renkin, 1988). This procedure is equivalent to removing all wavelengths greater than 4000 km, tapering between 4000 and 1600 km and retaining all the geoid anomalies with wavelengths shorter than 1600 km.

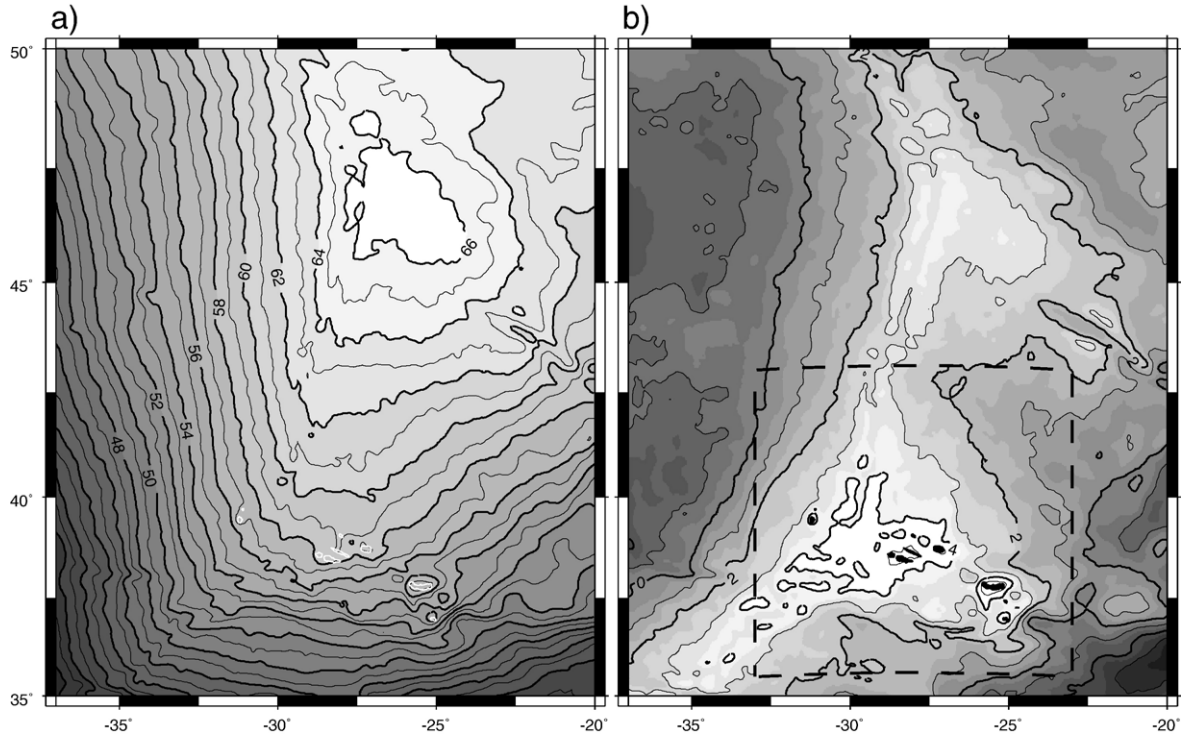

Fig. 6. a) Geoid anomaly map for a region enclosing the Azores Plateau from Sandwell and Smith's 2-min geoid grid; b) residual geoid heights calculated by removing all wavelengths greater than 4000 km, tapering between 4000 and 1600 km and retaining all the geoid anomalies with wavelengths shorter than 1600 km. The filtering was done using the EGM96 model.

Fig. 6 displays the geoid anomalies before and after filtering. Although the Azores Plateau is marked by a prominent bathymetric anomaly, its effect in terms of geoid is completely masked out by the main anomaly centered at 47°N (Fig. 6a). Filtering brings out evidence of the geoid anomaly belonging to the Azores tectonic province and centered at approximately 38°N (Fig. 6b). The dashed rectangle delimits the area inside which the admittance analysis was performed.

Geoid and bathymetry can be corrected for the thermal cooling effect of the oceanic lithosphere assuming an half-space cooling model. We performed these corrections considering that the geoid anomaly decreases at a rate of 0.16 m/Ma (Turcotte and Schubert, 2002, Eq. 5-157), that the seafloor subsides according to the square root of age (Turcotte and Schubert, 2002, Eq. 4-209), and using the ocean floor age determined from the digital map by Muller et al. (1997). However, the coherence of the corrected geoid and bathymetry is less than 0.5 for wavelengths larger than 100 km (Fig. 7, dashed line). This means that in the medium- to long-wavelength range, the age-corrected geoid is poorly correlated with the bathymetry and therefore the admittance cannot be considered meaningful. This is hardly surprising considering that the assumptions of the half-space cooling model are not fully met in the Azores. Whatever originated the volcanism that built the islands and the many submarine volcanoes that populate the Plateau, it may have re-heated the lithosphere and reset the clock of the geoid age variation. This resetting might very well explain why the age corrections lead to such a poor coherence.

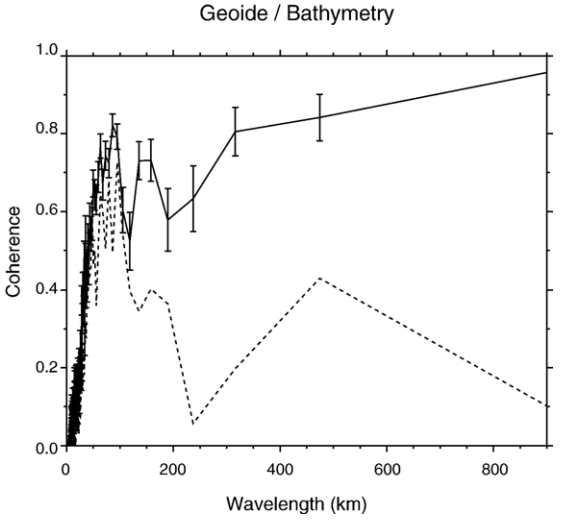

Fig. 7. Coherence of geoid and bathymetry before (solid line) and after (dashed line) correction of age-dependent cooling. The low coherence of the corrected geoid and bathymetry is attributed to the inadequacy of the half-space cooling model for the Azores region.

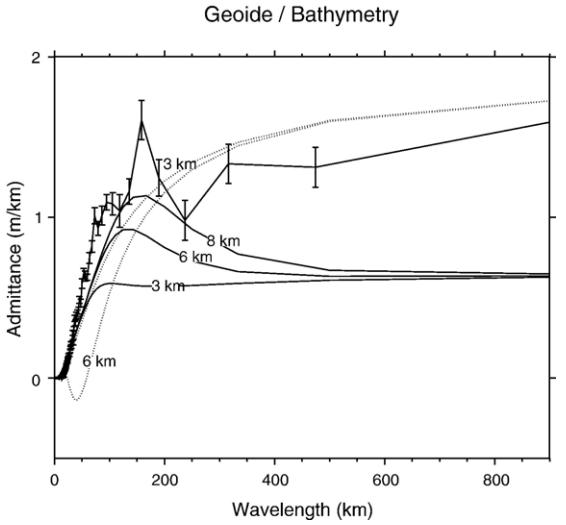

Fig. 8. Geoid to bathymetry admittance. The observed admittance (solid thick line) is shown with error bars representing ±1 σ. Theoretical bottom-load models are represented by dotted lines and theoretical top-load models by solid lines. Values of 3, 6 and 8 km indicate the model elastic thickness. The compensation depth assumed for the bottom load is 25 km.

In contrast, the non-corrected geoid (Fig. 7, solid line) is highly correlated with bathymetry for wavelengths larger than 50 km. Based on the coherence results, we use the non-corrected geoid to compute the admittance, according to Eq. (7). The computed admittance and correspondent error bars are plotted in Fig. 8. Also shown are the theoretical transfer functions for (1) "load on top" models assuming elastic thicknesses of 3, 6 and 8 km (solid lines), and (2) "load from below" models assuming a mean depth of load of 25 km and elastic thicknesses of 3 and 6 km (dotted lines).

A model of loading from below with an elastic thickness of 3 km and a mean depth of load of 25 km is the one that best fits the geoid admittance results (Fig. 8). Other models (not shown) of loading from below with larger elastic thickness and deeper loads over predict the admittance for wavelengths larger than ~150 km, while those with larger elastic thickness and shallower loads under predict the admittance for wavelengths shorter than ~150 km.

Under the hypothesis of local isostatic compensation, which can be assumed at wavelengths much greater than the flexural wavelength, the geoid is linearly related to the bathymetry (Ockendon and Turcotte, 1977). For wavelengths between 600 and 4000 km, Sandwell and Renkin (1988) noted that the transfer functions Z_{Top} and Z_{Bot} could be approximated by a constant value, and proposed that isostasy could be studied using the geoid to bathymetry ratio (N/B) in the space domain instead. According

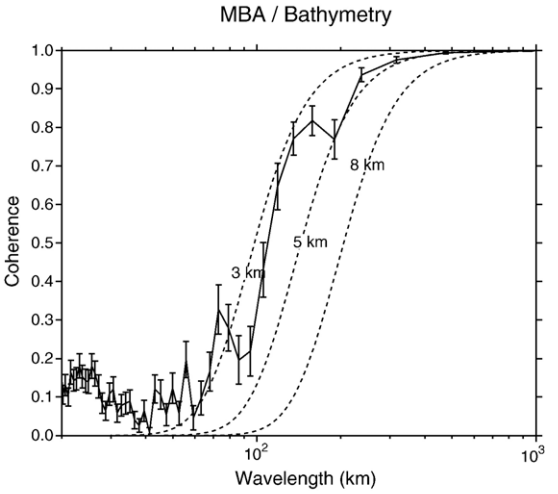

Fig. 9. Coherence of MBA to bathymetry (solid line) as a function of wavelength. Dashed curves show the coherence predicted for elastic models with combined loading, assuming plate thicknesses of 3, 5, and 8 km, and equal loading at the surface and at the Moho. The Moho is assumed to occur at an average depth of 12 km below the seafloor.

to this method, a low geoid/bathymetry ratio (<2 m/km) means shallow Airy compensation, an intermediate ratio (2–6 m/km) corresponds to thermal isostasy and/or dynamic uplift from a mantle plume, and a high ratio (>6 m/km) indicates compensation by density anomalies beneath the lithosphere that are dynamically maintained by mantle convection (Sandwell and Renkin, 1988; Sandwell and MacKenzie, 1988).

Fig. 8 shows that, in the long-wavelength range (>600 km), the admittance has a nearly constant value of ~1.6 m/km. This is similar to the N/B ratio of 1.4 m/km achieved by Grevemeyer (1999) in a space–domain study of the Azores region. Therefore, our results indicate thickened crust and Airy compensation, and consequently do not support the hypothesis that the Azores Plateau is caused by a thermal swell and/or dynamic uplift by a mantle plume.

6. MBA to bathymetry

The MBA is calculated by subtracting from the free air anomaly the gravity effect of the water/crust and crust/mantle interfaces assuming a crust of constant thickness. It represents the gravity field after water and crust have been replaced by mantle rock and reveals either variations in crustal density or departures of the crustal thickness from an average value. Following Kuo and Forsyth (1988) we use the method of Parker (1972) to convert topography and constant density contrasts to gravity anomalies. The Moho is assumed to lie at an average depth of 12 km below the seafloor and to follow the seafloor topography. The densities assumed for water, crust and mantle are listed in Table 1.

The coherence between MBA and bahymetry is displayed in Fig. 9 as a function of wavelength. Note that the wavelength axis is now logarithmic instead of linear. Coherence values near unity in the long-wavelength range indicate local (Airy) isostasy, in which none of the bathymetry is supported by the flexural strength of the lithosphere. Low coherence on the other hand may indicate that surface loading due to bathymetry and subsurface loading due to internal density contrasts are statistically independent processes, decoupled from the elastic plate (Forsyth, 1985). At short wavelengths (<50 km), the low coherence is attributed to the presence of noise. The wavelength of the transition from high to low coherence provides an indication of the flexural rigidity of the lithosphere.

The theoretical coherence of the MBA with bathymetry is computed as function of wavelength from Eq. (5), assuming that surface and subsurface loading are statistically uncorrelated and that $F=1$ (i.e., equal loading at the surface and at the Moho). Fig. 9 shows that the observed coherence (solid line) lies between the theoretical curves representing elastic models with $T_e=3$ km and $T_e=5$ km (dashed lines). The breadth of the transition from high to low coherence suggests that the elastic thickness is not constant over the region, probably varying between 3 and 5 km. Such range of

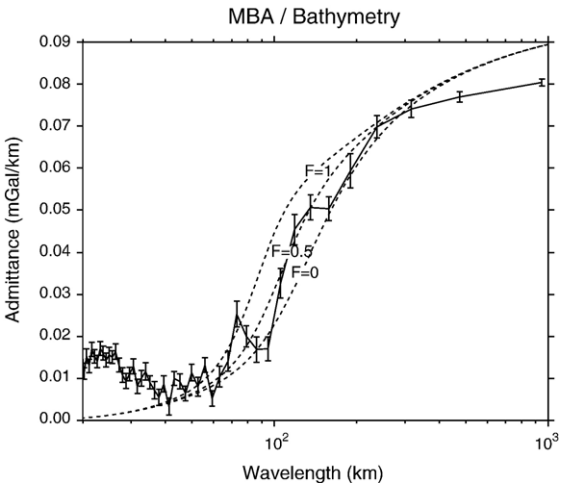

Fig. 10. MBA to bathymetry admittance considering both loading on top and loading from below. The dotted line with stars represents the observed admittance, and the solid lines the theoretical functions. Theoretical models assume an elastic plate 5 km thick and a Moho depth below sea level of 12 km. The initial amplitude ratio of the bottom to top load is displayed for $F=0$, 0.5 and 1.

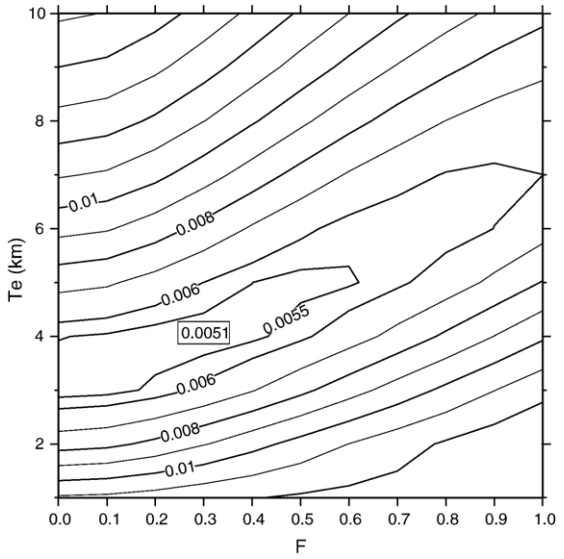

Fig. 11. RMS plot of the misfit between the theoretical and observed admittance between MBA and bathymetry, as a function of elastic thickness (T_e) and ratio of bottom to top loading (F).

elastic thickness agrees with the result of the FAA to bathymetry admittance analysis.

Next we compute the admittance between the MBA and the bathymetry, shown in Fig. 10 (solid line). For models of combined loading, the theoretical admittance between the MBA and the bathymetry is a function of T_e and F (see Eq. (4)). Theoretical admittance curves for T_e=5 km and three different F ratios (0, 0.5 and 1) are plotted in Fig. 10 to illustrate the effect of changing the ratio of bottom to top loading. The observed admittance is clearly higher than that predicted by surface loading only (F=0), demonstrating the presence of a component of subsurface load.

The parameters T_e and F can be better constrained using rms-misfit analysis, as shown in Fig. 11. The value of the elastic thickness was systematically varied between 1 and 10 km and the ratio of bottom to top loading varied between 0 and 1. For each model the rms-misfit calculation between the observed and theoretical admittance was restricted to wavelengths larger than 50 km. The misft plot shows a minimum for T_e=4 km and F=0.3. This means that the component of subsurface load at the Moho has an amplitude of about 1/3 of the component of surface load caused by topography. Previous studies that neglected subsurface loading estimated that the average elastic thickness in the Azores region was about 7–8 km (Luis et al., 1998). Including the presence of shallow loading at the Moho brings this estimate to 4 km and leads to an isostatic model that is consistent both with geoid and gravity data.

7. Discussion and conclusions

The analysis of the geoid to bathymetry admittance suggests that the elastic plate underneath the Azores Plateau has such low rigidity (T_e=3 km) that the compensation mechanism resembles Airy. Accordingly, the compensation of the Plateau is mainly achieved through crustal thickening. The average depth of compensation is relatively shallow, about 25 km in depth, but top and bottom loads cannot be discriminated in this case. Thus, at long wavelengths, the relative importance of surface and subsurface loading has no physical significance, and bottom loads are undistinguishable from surface loads (Forsyth, 1985). We find no sign of mantle plume upwelling or thermal isostasy involving lithosphere thinning. Considering that hotspots are presumed to be hot plumes that come from deep in the mantle (Wilson, 1963) our results do not corroborate the hypothesis that geophysical and tectonic anomalies in the Plateau (e.g., shallow bathymetry, geoid anomalies, abundant off-axis volcanism and migrating plate boundaries) are due to the Azores hotspot and its interactions with the MAR.

If the Azores swell is associated with deep-seated (100–200 km depth) thermal/density anomalies beneath the lithosphere (Zhang and Tanimoto, 1993), we would expect a significantly larger geoid to bathymetry ratio than what we obtain. In fact, the existence of lower-mantle heterogeneities beneath the Azores cannot be regarded as evidence for dynamic topography, because many of the lower-mantle heterogeneities mapped by tomography are not reflected in the surface topography (e.g., Bercovici et al., 2000). We prefer the hypothesis that the Azores volcanism and the associated swell, rather than being created by a hotspot, is the result of tectonic and magmatic processes related to triple-junction migration.

Our results of the Free air gravity to bathymetry admittance are more conclusive in the wavelength range of the flexural response of the lithosphere (<400 km). We find that a model in which the plate deflects in response to surface topographic loads, with an effective elastic thickness in the range between 3 and 6 km, applies to the Azores Plateau. A lower limit of 3 km is not too low considering that our region of study includes the MAR. Indeed very low values of elastic thickness have been found in the vicinity of the MAR and elsewhere near mid-ocean ridges, for instance 2 km along a 10 km wide zone centered on the MAR at 31–36°S (Neumann and Forsyth, 1993), 1.6 km over the Amsterdam–St. Paul Plateau near the Southeast Indian Ridge (Scheirer et al., 2000) and 5–3 km underneath the

young Foundation Seamounts near the Pacific–Antarctic Ridge (Maia and Arkani-Hamed, 2002).

The best-fitting compensation model is that of an elastic plate on average 4 km thick, deflecting downwards in response to surface volcanic loads and upwards in response to negative loads applied at the Moho. The model is predominantly loaded on top, with a ratio of initial amplitude of subsurface to surface load of 0.3. Loads at the Moho, predicted at 12 km depth, can occur either by lateral variations in density or by relief of the density interface. Negative loading at relatively shallow depths, associated to enhanced crustal production, may be due to the emplacement of subsurface plutons.

Thus, we propose that focused mantle upwelling triggered from above by extensional stresses and plate discontinuities lead to the accretion of large volumes of extrusives accompanied by crustal growth in the form of underplating. Crustal underplating consisting of material added at the base of the crust, lighter than mantle but with a higher than normal lower-crustal seismic velocities, can induce buoyant forces that account for anomalously high topography (e.g., Ito and Clift, 1998; Grevemeyer and Flueh, 2000). Underplating in the Azores is suggested by a Rayleigh-wave dispersion study based on earthquakes recorded in S. Miguel, which indicated that the upper mantle seismic velocities beneath the Plateau are anomalously low (Searle, 1976). In addition, depth–velocity models in the Azores indicate velocities of ~ 7.5 km/s (between those of lower-crustal mafic rocks and upper mantle ultramafic rocks) at depths below 8–11 km (Hirn et al., 1980; Miranda et al., 1988).

However, by comparing our ratio of bottom to top loading to that of other studies (e.g., Grevemeyer et al., 2001) we are forced to conclude that the extent of underplating in the Azores must be small. Following an admittance analysis in the Ninetyeast ridge, Grevemeyer and Flueh (2000) found a ratio of subsurface to surface load slightly larger than 0.5. A seismic survey in the region allowed mapping of the shape of the volcanic edifice and the extent of the underplated material. Based on this seismic model, the volume ratio between the mafic/ultramafic underplate and extrusive/intrusive rocks was constrained to be about 0.7 (Grevemeyer et al., 2001). This is somewhat higher than the 0.3 ratio we obtain for the Azores; yet, the maximum thickness of underplated body in the Ninetyeast ridge is 5 km under the center of the extrusive/intrusive edifice.

It would be advantageous to use the coherence of free air gravity and/or geoid to bathymetry to estimate the simultaneous presence of top and bottom loads, as well as the depth of compensation of the bottom load. In order to do so a theoretical coherence for combined loading needs to be derived, in the same way Forsyth (1985) derived the coherence using the MBA anomaly. The restriction of the bottom load being applied at the Moho could then be released. We speculate that the drop in coherence observed in Figs. 5 and 7 at wavelengths of about 200 km is due to the existence of a top load as well as a bottom load. Since the wavelength range of the transition from low to high coherence depends on the elastic thickness and on the load type (top, bottom or both) we anticipate that the observed drop can be predicted by theoretical functions.

Acknowledgements

We wish to thank Pascal Gente for allowing us to use his new bathymetric grid. Thanks to Walter Smith for his help on the development of part of the computer code used in this work and also for the helpful discussions. We thank to Ingo Grevemeyer and an anonymous reviewer for the valuable comments that improved the manuscript. This work was supported by the PDCTM STAMINA (3/3.1/CEG/2619/95) project.

References

Asimow, P.D., Langmuir, C.H., 2003. The importance of water to oceanic mantle melting regimes. Nature 421, 815–820.

Banks, R., Parker, R., Huestis, S., 1977. Isostatic compensation on a continental scale: local versus regional mechanisms. Geophys. J. R. Astron. Soc. 51, 431–452.

Bendat, J.S., Piersol, A.G., 2000. Random Data Analysis and Measurement Procedures, 3rd edition. John Wiley.

Bercovici, D., Ricard, Y., Richards, M., 2000. The relation between mantle dynamics and plate tectonics: a primer. The History and Dynamics of Global Plate Motions. Geophysical Monograph, vol. 21. AGU.

Bonatti, E., 1990. Not so hot "hot spots" in the oceanic mantle. Science 250, 107–110.

Cannat, M., Briais, A., Deplus, C., Escartin, J., Georgen, J., Lin, J., Mercuriev, S., Meyzen, C., Muller, M., Pouliquen, C., Rabain, A., Silva, P., 1999. Mid-Atlantic Ridge–Azores hotspot interactions: along-axis migration of a hotspot-derived event of enhanced magmatism 10 to 4 Ma ago. Earth Planet. Sci. Lett. 173, 257–269.

Cazenave, A., Dominh, K., Rabinowicx, M., Ceuleneer, G., 1988. Geoid and depth anomalies over ocean swells and troughs: evidence of increased trend of geoid age ratio with plate age. J. Geophys. Res. 93, 8064–8077.

Dorman, L.M., Lewis, B.T.R., 1970. Experimental isostasy, 1, theory of the determination of the earth's isostatic response to a concentrated load. J. Geophys. Res. 75, 3357–3375.

Féraud, G., Kaneoka, I., Allègre, J.C., 1980. K/Ar ages and stress pattern in the Azores: geodynamic implications. Earth Planet. Sci. Lett. 46, 275–286.

Forsyth, D.W., 1981. Can the strength of the lithosphere be inferred from the average relationship between the topography and gravity anomalies. EOS Trans., AGU 62, 1032 (abstract).

Forsyth, D.W., 1985. Subsurface loading and estimates of the flexural rigidity of continental lithoshere. J. Geophys. Res. 90, 12623–12632.

Gente, P., Dyment, J., Maia, M., Goslin, J., 2003. Interactions between the MAR and the Azores hot spot during the last 85 Myr: emplacement and rifting of the hot spot-derived plateaus. G-cube 4, 1–23.

Grevemeyer, I., 1999. Isostatic geoid anomalies over mid-plate swells in the Central North Atlantic. Geodynamics 28, 41–50.

Grevemeyer, I., Flueh, E.R., 2000. Crustal underplating and its implications for subsidence and state of isostasy along the Ninetyeast Ridge hotspot trail. Geophys. J. Int. 142, 643–649.

Grevemeyer, I., Flueh, E.R., Reichert, C., Bialas, J., Klaschen, D., Kopp, C., 2001. Crustal architecture and deep structure of the Ninetyeast Ridge hotspot trail from active-source ocean bottom seismology. Geophys. J. Int. 144, 414–431.

Heller, D.-A., Marquart, G., 2002. An admittance study of the Reykjanes Ridge and elevated plateaux between the Charlie–Gibbs and Senja fracture zones. Geophys. J. Int. 148, 65–76.

Hirn, A., Haessler, H., Hoang Tronc, P., Wittlinger, G., Mendes Victor, L.A., 1980. Aftershock sequence of the January 1, 1980, earthquake and present-day tectonics in the Azores. Geophys. Res. Lett. 7, 501–504.

Ito, G., Clift, P.D., 1998. Subsidence and growth of Pacific Cretaceous plateaus. Earth Planet. Sci. Lett. 161, 85–100.

Ito, G., Lin, J., 1995. Oceanic spreading center–hotspot interactions: constraints from along-isochron bathymetric and gravity anomalies. Geology 23, 657–660.

Karner, G.D., Watts, A.B., 1983. Gravity anomalies and flexure of the lithosphere at mountain ranges. J. Geophys. Res. 88, 10449–10477.

Klitgord, K.D., Schouten, H., 1986. Plate kinematics of the Central Atlantic. In: Vogt, P.O., Tucholke, B.E. (Eds.), The Geology of the North America, the Western North Atlantic Region. Vol. M. Geol. Soc. Am., Boulder, Colorado, pp. 351–378.

Kuo, B-Y., Forsyth, D., 1988. Gravity anomalies of the ridge-transform system in the South Atlantic between 31° and 34.5°S: upwelling centers and variations in crustal thickness. Mar. Geophys. Res. 10, 205–232.

Lemoine, F.G., Kenyon, S.C., Factor, J.K., Trimmer, R.G., Pavlis, N.K., Chinn, D.S., Cox, C.M., Klosko, S.M., Luthcke, S.B., Torrence, M.H., Wang, Y.M., Williamson, R.G., Pavalis, E.C., Rapp, R.H., Olsen, T.R., 1998. The development of the joint NASA GSFC and the National Imagery and Mapping Agency (NIMA) geopotential model EGM96. Report no. NASA/TP-1998-206861. National Aeronautics and Space Administration.

Louden, K.E., 1981. A comparison of the isostatic response of bathymetric features in the north Pacific Ocean and the Philippine Sea. J. Geophys. Res. 64, 393–424.

Lourenço, N., Luis, J.F., Miranda, J.M., Ribeiro, A., Mendes Victor, L.A., 1988. Morpho-tectonic analysis of the Azores Volcanic Plateau from a new bathymetric compilation of the area. Mar. Geophys. Res. 20, 141–156.

Luis, J.F., Miranda, J.M., Galdeano, A., Patriat, P., Rossignol, J.C., Victor, L.A., 1994. The Azores triple junction evolution since 10 Ma from aeromagnetic survey of the Mid-Atlantic Ridge. Earth Planet. Sci. Lett. 125, 439–459.

Luis, J.F., Miranda, J.M., Galdeano, A., Patriat, P., 1998. Constraints on the structure of the Azores spreading center from gravity data. Mar. Geophys. Res. 20, 156–170.

Maia, M., Arkani-Hamed, J., 2002. The support mechanism of the young Foundation Seamounts inferred from bathymetry and gravity. Geophys. J. Int. 149, 190–210.

McKenzie, D., Bowin, C., 1976. The relationship between bathymetry and gravity in the Atlantic Ocean. J. Geophys. Res. 81, 1903–1915.

McNutt, M., 1979. Compensation of oceanic topography, an application of the response function technique to the Surveyor area. J. Geophys. Res. 84, 7589–7598.

McNutt, M., 1983. Influence of plate subduction on isostatic compensation in northern California. Tectonics 2, 399–415.

Miranda, J.M., Mendes Victor, L.A., Simões, J.Z., Luis, J.F., Matias, L., Shimamura, H., Shiobara, H., Nemoto, H., Mochizuki, H., Hirn, A., Lépine, J.C., 1988. Tectonic setting of the Azores Plateau deduced from a OBS survey. Mar. Geophys. Res. 20, 171–182.

Monnereau, M., Cazenave, A., 1990. Depth and geoid anomalies over oceanic hotspot swells. A global survey. J. Geophys. Res. 95, 15429–15438.

Morgan, W.J., 1971. Convection plumes in the lower mantle. Nature 230, 42–43.

Muller, R.D., Roest, W.R., Royer, J.-Y., Gahagan, L.M., Sclater, J.G., 1997. Digital isochrons of the world's ocean floor. J. Geophys. Res. 102, 3211–3214.

Neumann, G.A., Forsyth, D.W., 1993. The paradox of the axial profile: Isostatic compensation along the axis of the Mid-Atlantic Ridge? J. Geophys. Res. 98, 17891–17910.

Ockendon, J.R., Turcotte, D.L., 1977. On the gravitational potential and field anomalies due to thin mass layers. Geophys. J. R. Astron. Soc. 48, 479–492.

Parker, R.L., 1972. The rapid calculation of potential anomalies. Geophys. J. R. Astron. Soc. 31, 447–455.

Sandwell, D.T., MacKenzie, K.R., 1988. Geoid height versus topography for oceanic plateaus and swells. J. Geophys. Res. 94, 7403–7418.

Sandwell, D.T., Renkin, M.L., 1988. Compensation of swells and plateaus in the North Pacific: no direct evidence for mantle convection. J. Geophys. Res. 93, 2775–2783.

Sandwell, D., Smith, W., 1997. Marine gravity anomaly from Geosat and ERS-1 satellite altimetry. J. Geophys. Res. 102, 10039–10054.

Sartoni, R., Torelli, L., Zitellini, N., Peis, D., Lodolo, E., 1994. Eastern segment of the Azores–Gibraltar line (central-eastern Atlantic): an oceanic plate boundary with diffuse compressional deformation. Geology 22, 555–558.

Searle, R., 1976. Lithospheric Structure of the Azores Plateau from Rayleigh-wave dispersion. Geophys. J. R. Astron. Soc. 44, 537–546.

Scheirer, D.S., Forsyth, D.W., Conder, J.A., Eberle, M.A., Hung, S.H., Jonhson, K.T.M., Graham, D.W., 2000. Anomalous seafloor spreading of the southeast Indian ridge near the Amsterdam–St. Paul plateau. J. Geophys. Res. 105, 8243–8262.

Schilling, J., 1975. Azores mantle blob: rare-earth evidence. Earth Planet. Sci. Lett. 25, 103–115.

Schilling, J., 1991. Fluxes and excess temperatures of mantle plumes inferred from their interaction with migrating mid-ocean ridges. Nature 352, 397–403.

Sclater, J.G., Lawer, L.A., Parsons, B., 1975. Comparison of long-wavelength residual elevation and free-air gravity anomalies in the North Atlantic and possible implications for the thickness of the lithospheric plate. J. Geophys. Res. 80, 1031–1052.

Smith, W.H.F., Sandwell, D.T., 1994. Bathymetric prediction from dense satellite altimetry and sparse shipboard bathymetry. J. Geophys. Res. 99, 21803–21824.

Smith, W.H.F., Sandwell, D.T., 1997. Global seafloor topography from satellite altimetry and ship depth soundings. Science 277, 1956–1962.

Srivastava, S.P., Tapscott, C.R., 1986. Plate kinematics of the North Atlantic. In: Vogt, P.O., Tucholke, B.E (Eds.), The Geology of the North America, the Western North Atlantic Region. Vol. M. Geol. Soc. Am., Boulder, Colorado, pp. 379–404.

Turcotte, D., Schubert, G., 2002. Geodynamics. Second ed. Cambridge University Press, pp. 456.

Watts, A., 1978. An analysis of isostasy in the world's oceans 1. Hawaiian–Emperor Seamount Chain. J. Geophys. Res. 83, 5989–6004.

Wilson, T., 1963. Mantle plumes and plate motions. Tectonophysics 19, 149–164.

White, W., Schilling, J., Hart, S., 1976. Evidence for the Azores mantle plume from strontium isotope geochemistry of the Central North Atlantic. Nature 263, 659–663.

Zhang, Y.-S., Tanimoto, T., 1993. High-resolution global upper mantle structure and plate tectonics. J. Geophys. Res. 98, 9793–9823.